VALIDATION OF HIGH-RESOLUTION SATELLITE RAINFALL PRODUCTS FOR RIVER FLOW PREDICTION IN NORTH AFRICA

H SAF Associated/Visiting Scientist activity

H_AVS20_02

Yves Tramblay

09/10/2021

1. INTRODUCTION

Data availability is essential for the monitoring of water resources and also to manage hydrological risks such as floods and droughts. As most African countries, North African countries have a low density of rainfall and river gauging stations and when data exist its availability is not always granted. As an alternative to ground-based observations, in recent decades, satellite products and reanalysis have increased their accuracy to reproduce different components of the hydrological cycle and notably precipitation with an almost global coverage. They have become increasingly available with adequate spatial and temporal resolution for hydrological applications in moderate to small size basins. This could provide a valuable alternative to the lack of ground measurements at national and regional scales.

Maghreb countries do not currently have operational scheme for the management of water resources or flood alerts systems, resulting in a strong vulnerability of agricultural productions to water availability and also a high human exposure the flooding that are causing twice as much fatalities than in northern Mediterranean countries. The major scientific challenges to implement such operational systems are the adaptation to the semi-arid context of the operational methods used in other regions such as Europe, as well as the lack of observed data. At European level, the EFAS system (European Flood Awareness System, www.efas.eu) is issuing hydrological alerts since 2012, based on a distributed hydrological model, LISFLOOD (Van der Knijff et al., 2010) forced by meteorological forecasts. At present, the model is already implemented in Africa but is not calibrated for the majority of basins (Thiemig et al., 2015), which greatly limits the usefulness of the system for providing forecasts. Within this context, a few attempts to develop hydrological modelling with remote sensing data in these regions have been made, taking advantage of the existing sparse datasets of precipitation measured at the ground and discharge (Tramblay et al., 2012, 2016; El Khalki et al., 2018, 2020, Saouabe et al., 2020). There is a growing interest in considering satellite

observations of precipitation to be incorporated in hydrological modelling approaches. However, as the outcomes may differ noticeably depending on the hydrological model used, the satellite-based precipitation product selected and the region considered (Nguyen et al. 2018), is not so trivial to draw general guidelines about which combination of satellite product and hydrological model should be favored. Furthermore, even if satellite precipitation errors can significantly influence the performance of a hydrological model, improving rainfall estimates through e.g., bias-correction methods do not systematically improve streamflow simulations (Beria et al. 2017).

The EUMETSAT H SAF (European operational satellite agency for monitoring weather, climate and the environment from space - Satellite Application Facility on Support to Operational Hydrology and Water Management) generates and distributes various satellite products (precipitation, soil moisture and snow) with the aim of support hydrological applications worldwide. H-SAF's high-resolution precipitation satellite products can be a valuable source of information of precipitation at different temporal and spatial scales for Maghreb River basins. Recent H-SAF products are characterized by different data acquisition techniques / sensors and by different spatial and temporal resolutions. These resolutions allow the forcing of hydrological models by these precipitation products to compensate for the lack of data in ungauged basins. In this study we tested six different precipitation products derived from: 1) The Integrated Multi-Satellite Retrievals, IMERG of the Global Precipitation Measurement Mission, GPM (Hou et al., 2014), 2) the rainfall estimated by applying the SM2RAIN (Soil Moisture to RAIN) algorithm to the soil moisture product ASCAT, SM2RAIN-ASCAT (Brocca et al., 2014) and 4) four different H SAF products (H03, H05, H64 and H67).

The objectives of this Associated/Visiting Scientist activities were twofold. The first task was to collect hydro-meteorological data for several river basins in North Africa, in order to be representative of different physiographic and climatic contexts. The second task was to evaluate the different satellite precipitation products, using either a statistical approach based on the correlation between rainfall and runoff events or different hydrological models to reproduce the rainfall-runoff relationships at the daily time scale. Four hydrological models are applied to evaluate the sensitivity of the results to different model formulations: IHACRES (Croke and Jakeman, 2004), MISDc (Brocca et al., 2013), GR4J (Perrin et al., 2003) and CREST (Wang et al., 2011).

2. DATASETS

2.1 Observed data in North African basins

This project focuses on the North African basins and more specifically Morocco, Algeria and Tunisia. During the course of the project, we were able to collect hydrometric data from 41 watersheds distributed as follows: 27 in Morocco, 4 in Algeria and 10 in Tunisia. The catchment boundaries have been delineated using the HydroShed 300 meters resolution digital elevation model (Figure 1). The basins have areas that vary between 0.78 km² and 16,051 km². The majority of the basins are formed by carbonate formations with rates of 45%, 37% and 49% respectively of surface coverage in Morocco, Algeria and Tunisia, representative of various ranges of soil infiltration capacity. Impermeable formations are mostly present in the basins of the High Atlas of Marrakech in South Morocco in the form of plutonic and metamorphic rocks. The time series of river discharge data covers an average period of 39 years with a minimum of 3 years and a maximum of 64 years. The data collected across the different countries sent went over scrutiny to detect potential spurious and missing data. This analysis revealed that many stations have gaps in the time series, of various lengths. Some examples of errors found in the time series are depicted in Figure 2, in many cases some time periods with missing data are wrongly reported as zero-flow days, that could strongly bias the analysis. Also, some obvious data errors have been detected for some periods when a linear gap-filling method has been employed by the data provider. Following this critical analysis, many stations with doubtful data have been discarded, in the absence of reliable metadata to document possible missing data or data points with a high uncertainty. To match the time period when all satellite precipitation products are available (see the next section) we only kept 12 basins, all located in Morocco, where complete daily time series of good quality are available during the time period 2014 to 2018 (Table 1).

In Table 1, we added some hydrological signatures relevant for representing the hydrological behavior of the different basins: the Richard-Baker flashiness index, defined as the sum of absolute differences between consecutive daily flows (Baker et al., 2004), the base flow index, that is the ratio between base flow and total streamflow, with base flow computed with

the standard UKIH (1980) method, the frequency of zero-flow days and the frequency of days with discharge below 0.1 $m^3.s^{-1}$ and the catchment areas. The two first signatures are proxies to estimate the level of aridity of the basins, with increased aridity the flashiness index is higher and base flow contribution lower. In addition, the frequency of zero-flow days and days below 0.1 $m^3.s^{-1}$ allow identifying the intermittent rivers that cease to flow during usually the summer period. It must be noted that the two frequencies differ, this is due to the difficulty to correctly estimate a true zero-flow day with rating curves, when very small computed discharge values may be considered as zero-flow days.
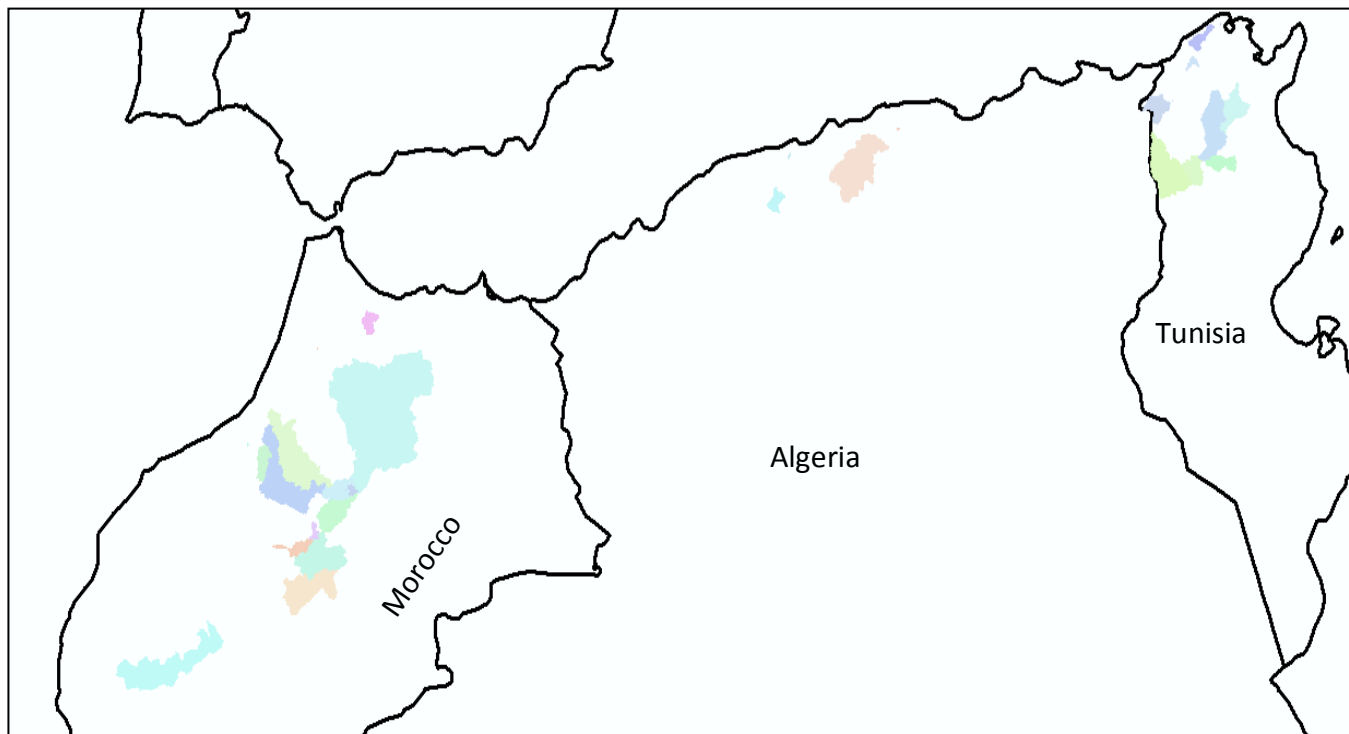

Figure 1: Location of the 41 basins where observed daily discharge data has been collected

Table 1: Selected stations where complete records of daily discharge data are available between 2014 and 2018

Name	Flashiness index	Base flow index	Freq_0	Freq_<0,1	Catchment area (km²)
AguibatZiar	0,452	0,300	2%	12%	3659,5
Ainloudah	0,707	0,267	53%	73%	698,3
Ait Ouchene	0,243	0,585	0%	0%	2402,5
Chachanmelah	0,326	0,506	0%	0%	1424,0
Lalla chafia	0,523	0,275	0%	13%	2234,9
Sidi_jabeur	0,737	0,137	13%	21%	3110,0
Sidi Mly Cherif	0,589	0,366	0%	56%	646,6
Taghzout	0,268	0,552	0%	20%	171,9
Tagzirt	0,566	0,263	0%	3%	531,9
Tamchachat	0,149	0,688	0%	14%	133,3
Terhat	0,128	0,818	0%	0%	1013,3
Tillouguite	0,167	0,664	0%	0%	2502,6

In addition to river discharge, we also had access to a large number of rainfall stations but only in the two countries (Morocco, 20 stations and Tunisia, 179 stations, see Figure S1) with a very heterogeneous spatial coverage. This ratio of spatial representativeness varies between 0.07 to 12.5km²/station for Morocco and between 0.48 to 7.89km²/station for Tunisia. This ratio is very high in Morocco, because the majority of large basins (area greater than 1000km²) have only a single precipitation station located at the outlet of the basin. On the other hand, the ratios are between 0.38 and 1 km²/station in the basins of central Morocco where the basin areas are under 500 km² and the number of stations in average is above 3 per basin. On average, the daily time series have a record length of 40 years. It should be noted that some very long records are available, such as 101 years for the Had Kourt station in

Morocco and 86 years for several basins in Tunisia. However, after initial data quality screening, it was found that most of the data is not relevant for the present work, since most of stations have data before the year 2010 or even 2000 for most stations in Tunisia. Moreover, the very strong spatial heterogeneity of station coverage prevents the calculation of reliable interpolated precipitation fields over the basins of interest. For these reasons, the observed precipitation data has not been considered in the present work.
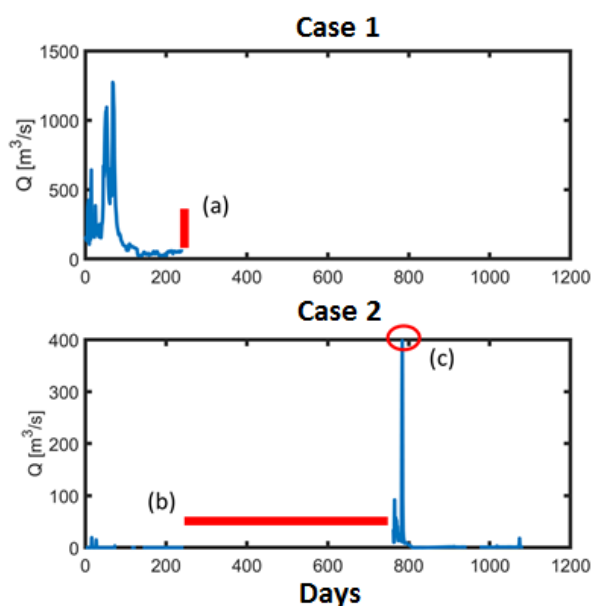
Figure 2: Example of two cases showing; (a) a very short time series with 0 discharge in place of missing data flags, (b) missing data wrongly reported as zeros and (c) an outlier

2.2 Satellite and Reanalysis products

After the selection of the river catchment collected for the analysis, the data for different satellite precipitation products described below have been extracted and averaged over each catchment.

2.2.1 GPM (Global Precipitation Measurement)

GPM is an international satellite product from NASA (National Aeronautics and Space Administration) and JAXA (Japan Aerospace Exploration Agency) available from April 2013. The GPM product brings together different satellite sensors with the IMERG algorithm (Intergrated Multi-satellite Retrievals GPM). GPM is the new generation of the TRMM

(Tropical Rainfall Measuring Mission) product which, after a great success that lasted 17 years, ended in April 2015. The particularity of the GPM product is that it is able to observe fine rain and snow by the use of a radar with two frequencies (13.6 GHz named KuPR and 35.5 GHz named KaPR) and a radar with multiple frequencies (10 GHz to 183 GHz) in order to understand the horizontal and vertical structure of precipitation. The KaPR frequency detects fine rain and snow and the KuPR detects intense rain which improve the detection of this type of rainfall event (Figure 3). The version 06 of GPM covers the period 2000-Present as it takes into account the TRMM measurements. This version has a temporal resolution of 30 min and spatial resolution of 0.1 ° x 0.1 ° and this, on a quasi-global coverage (65 ° N to 65 ° S). Three types of products are available depending on the level of correction of the observation:

1. Early: 4 hours after the time of observation: constitutes the raw observation of the satellite. Therefore, this version is also suitable for operational applications related to flood and landslide risk mitigation (Hou et al., 2014), this is the type of data considered in the present work.
2. Late: 14 hours after the time of the observation, which allows adding an observation of another satellite of the GPM constellation which is not taken into account in the Early version.
3. Final: 3 to 5 months after the time of observation. This version includes a climatological adjustment that incorporates GPCC gauge data
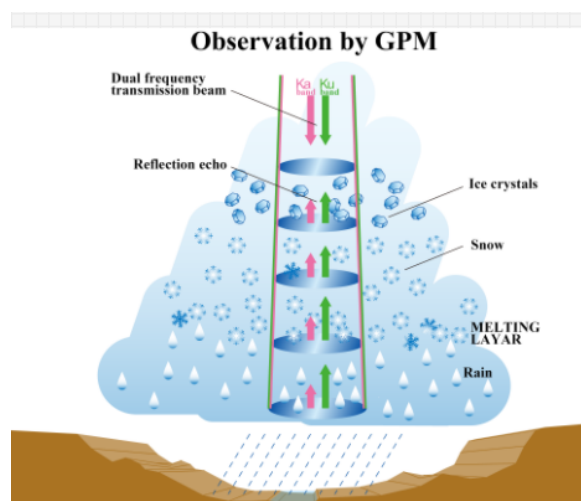
2.2.2 SM2RAIN

SM2RAIN is an innovative 'Bottom-Up' approach, developed by Brocca et al., 2014. It estimates rainfall from in-situ or satellite measurements of soil moisture. This algorithm has been applied to several satellite soil moisture products and has been shown to be effective in estimating daily rainfall (Brocca et al., 2014). The SM2RAIN product considered herein is based on the ASCAT (Advanced Scatterometer) satellite soil moisture with a daily time step and a spatial resolution of 12.5 km. The product covers the period 2007-2020 and is available at: http://hydrology.irpi.cnr.it/download-area/sm2rain-data-sets

2.2.3 H03

H03 (P-IN-GRU-SEVIRI) is a HSAF product based on infrared images captured by the SEVIRI instrument on Meteosat satellites. The product is generated every 15 min with a spatial resolution of 3 km. This resolution decreases with distance from the nadir until it reaches 8 km at the poles.

2.2.4 H05

H05 (P-AC-G-SEVIRI) is another H SAF product, based on the combination of LEO MW measurements and from GEO infrared images. The H05 product is generated and provided every 3 hours (00, 03, 06, 09, 12, 15, 18, 21 UTC). The integration periods for mixed MW + IR measurements at 15 min intervals (P-IN-GRU-SEVIRI) are the previous 3, 6, 12 and 24 hours. For this analysis the product provided every 24 hours at 00 UTC has been considered, in order to obtain daily rainfall estimates. The quality of the product depends on the type of precipitation and the integration period of the MW + IR measurements (Figure 5).
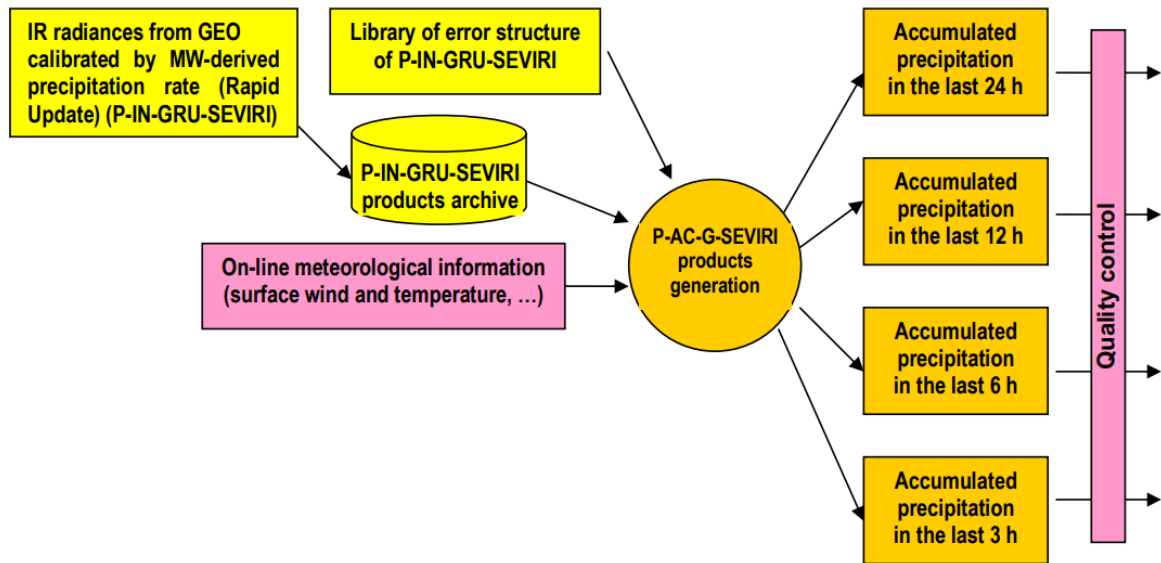
Figure 4: The steps for preparing the H05 product

2.2.5 H64

H64 is a precipitation product based on the integration of rainfall estimated through two different approaches. The algorithm combines rainfall estimates, obtained by the application of the SM2RAIN algorithm to satellite soil moisture products H101 and H16, and a passive microwave (PMW) product already operating on the H SAF Extended Area. The integration of the two estimations gives a product with greater accuracy and better performance which could be considered as a valid input to early warning systems for flood forecasting or other natural risks. The product is developed within the H SAF project by CNR IRPI in collaboration with CNR ISAC. The product is provided daily with a spatial resolution of 0.25° for the period 2014-2019

2.2.6 H67

H67 is a level 3 PMW H SAF product based on instantaneous precipitation measurement. It is available from product H68, giving a cumulative precipitation of 24 hours. This daily total is calculated from the cumulative precipitation every 6 hours (00, 06, 12, 18h UTC). The product has a spatial resolution of 0.25x0.25 ° and it covers the period 2014- Present.

2.2.7 ERA5

In addition to rainfall, the different hydrological models applied in the present work requires evapotranspiration as input in addition to rainfall data. Here, the potential evapotranspiration (PET) is computed from daily minimum and maximum air temperature from ERA5 using the Hargreave-Samani equation, that was found efficient to compute PET in North Africa (Er Raki et al., 2010). ERA5 (Copernicus Climate Change Service, C3S, 2017) is the most recent reanalysis of ECMWF (European Center for Medium Range Weather Forecasts). It combines meteorological reanalysis data produced by the combination of satellite measurements, ground observations or data assimilation. This grouping of information makes it possible to arrive at a more realistic representation of weather phenomena. ERA5 covers a period from 1950 to 2021 with a latency of 4 months, with spatial and temporal resolutions of 30 km and 1 hour respectively. Precipitation and temperature data were downloaded from the site: https://cds.climate.copernicus.eu.

3. METHODS

Two distinct but complementary approaches are considered to evaluate the ability of the different precipitation products to estimate river runoff. The first approach is data-driven and is based on the correlation between runoff events and cumulative rainfall preceding these events. The second approach is based on the calibration of hydrological models using satellite precipitation inputs, to identify the most suitable products at reproducing daily discharge dynamics.

3.3 Event-based analysis

The event-based analysis is first based on the identification of individual runoff events (ie. the unitary response of runoff to rainfall events) and then the correlation between the maximum runoff of each event with the corresponding rainfall. To avoid the detection of false events caused by small runoff fluctuations, only events with peak discharge higher than the 10% percentile of runoff were considered as potential events (Tarasova et al., 2019). Runoff events with no recorded precipitation the previous days are discarded. All daily values above a threshold (here we consider as thresholds the median and 95th percentile) are extracted from the time series of discharge. Then, to avoid introducing an autocorrelation signal in the

analysis, since runoff time series usually exhibit serial correlation event at the daily time step, a de-clustering approach has been applied to identify single events (see Figure 5). The de-clustering approach considered here is the standard approach of Lang et al., 1999 that apply two rules:

1- a minimum of n days between events, with n = 5 + log(catchment area)
2- between two consecutive peaks, runoff must drop below ⅔ of the smallest peak

After de-clustering, the maximum daily runoff of each event is kept. From this set of runoff events, the n-day previous precipitation is extracted. Event-based rainfall is estimated by a cumulative sum of precipitation before an event, the count stops if a day has zero precipitation. Finally, the correlation coefficient (Spearman) is computed between antecedent rainfall and the maximum event runoff.
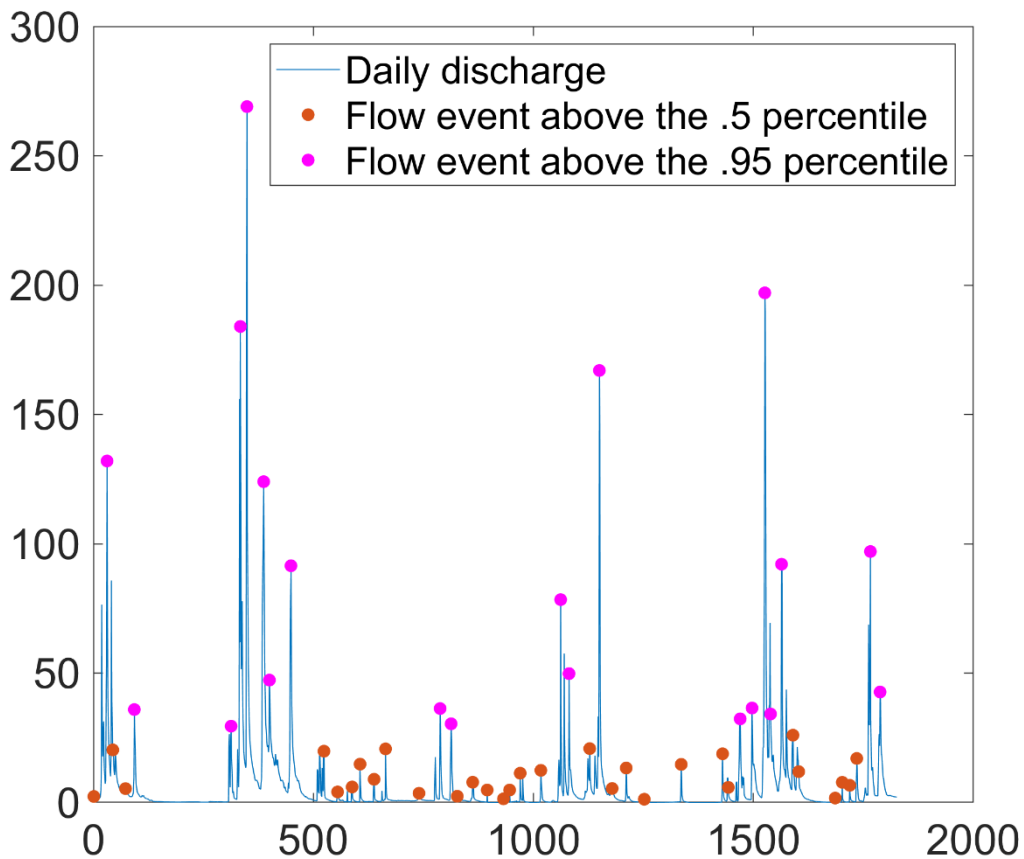
Figure 5: Example of runoff event identification, considering either the median or the 95th percentile as threshold for event detection

3.2 Hydrological modelling

This second approach consists in calibrating the parameters of four hydrological models (IHACRES, MISDc, GR4J and CREST) with the different precipitation products (GPM, SM2RAIN, H03, H05, H64 and H67) as input. The rationale of using different hydrological models is to evaluate to what extent the results could be dependent on the model structure, with different number of parameters and conceptualization of the rainfall-runoff transformation processes. For all models, the ERA5-derived PET is used in combination with precipitation. All models are calibrated using the same algorithm, the simplex search method, a direct search method that does not use numerical or analytic gradients. A transformation has been applied to the method to admit bound constraints to the model parameters. The bounds are applied using a transformation of the variables, they are inclusive inequalities, which admit the boundary values themselves, but will not permit any function evaluations outside the bounds. The simplex-based calibration method has been previously compared to more complex ones, such as the Shuffled Complex Evolution or Genetic algorithms, with fully comparable results and slower computational time, due to the limited dimensionality of the optimization problem herein. A calibration with bounded parameters is necessary since some compensation effects may occur with biased rainfall products, resulting in unfeasible hydrological model parameter values (Thiemig et al., 2013). Calibration results are evaluated by the KGE criterion (Kling et al., 2012) calculated between the observed and simulated flow rates. The KGE is a linear combination of three components of the modelling error: (i) the Pearson correlation coefficient, evaluating the error in shape and timing between observed (Qo) and simulated (Qs) flows, (ii) the bias between observed and simulated flows and (iii) the ratio between the simulated and observed standard deviations, evaluating the flow variability error.

3.2.1 IHACRES

In IHACRES, a non-linear model converts rainfall to effective rainfall by taking into account evapotranspiration and infiltration capacity (Croke and Jakeman, 2004), which gives the saturation state of the watershed for each time step (Figure 8). The nonlinear loss model has 3 parameters. The actual rain is then converted into flow following two parallel storage reservoirs. The two linear models use a time discretization, a transfer model and a unit

hydrograph representation. Finally, the simulated runoff is the sum of the fast and slow flow components. The aim of the IHACRES model is to characterize the hydrological behavior of a watershed using a reduced number of parameters (5 parameters in the current version, described in Table 2). The model has been also successfully applied in arid regions and was designed in Australia for regionalization purposes. In this study, we used the classic version of this IHACRES model (Croke and Jakeman, 2004).
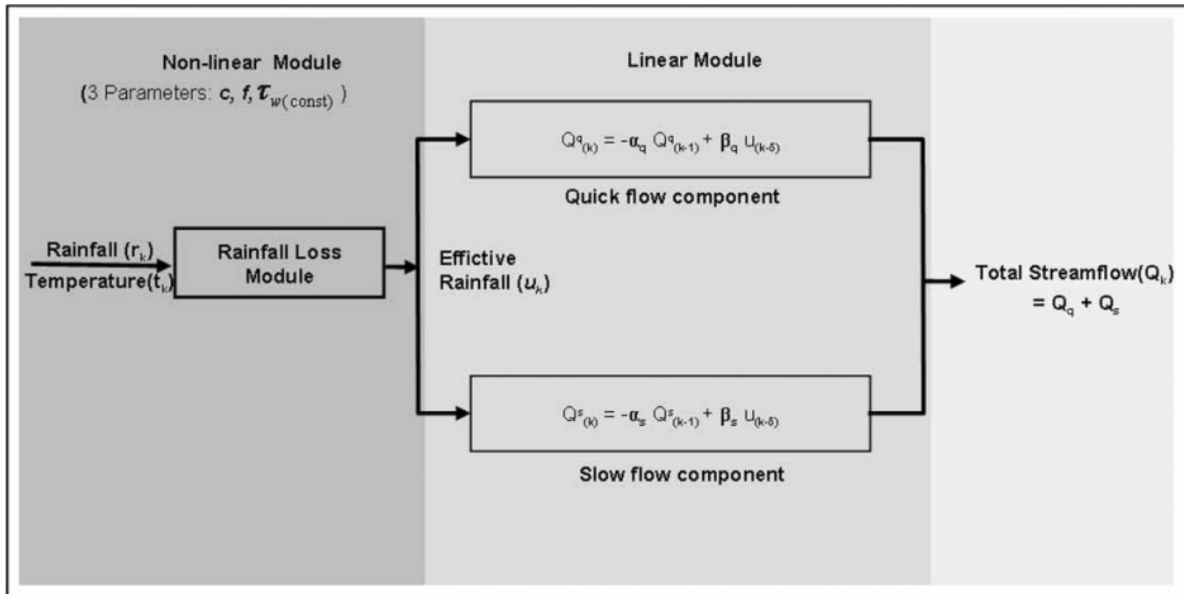

Figure 6: Structure of the IHACRES model

Table 2: Description of the parameters of the IHACRES model

Parameters	Description	Unit	Range of values
f	Catchment soil moisture deficit stress threshold as a function of d	-	[0.1 1.4]
Tau_s	Time constant for slow flow store	Days	[5 500]
Tau_q	Time constant for quick flow store	Days	[0.5 5]
V_q	Fractional volume for quick flow	-	[0 0.9]

d	Flow threshold	Mm	[20 800]

3.2.2 MISDc

The MISDc model (Modello Idrologico Semi-Distribuito in continuo, Brocca et al. (2011) (https://github.com/IRPIhydrology/MISDc) is a continuous hydrological model (Figure 7). The model simulates the different processes involved in the transformation of rain into flow (Infiltration, Evapotranspiration, excess soil saturation and percolation). Two components constitute the MISDc model; the first is the soil water balance model (Brocca et al., 2008) which simulates soil moisture for each time step and estimates the initial state of soil saturation. The second component continuously simulates the hydrograph. The version considered here is the one-layer model, it has a total of 8 parameters to be calibrated (Table 3).
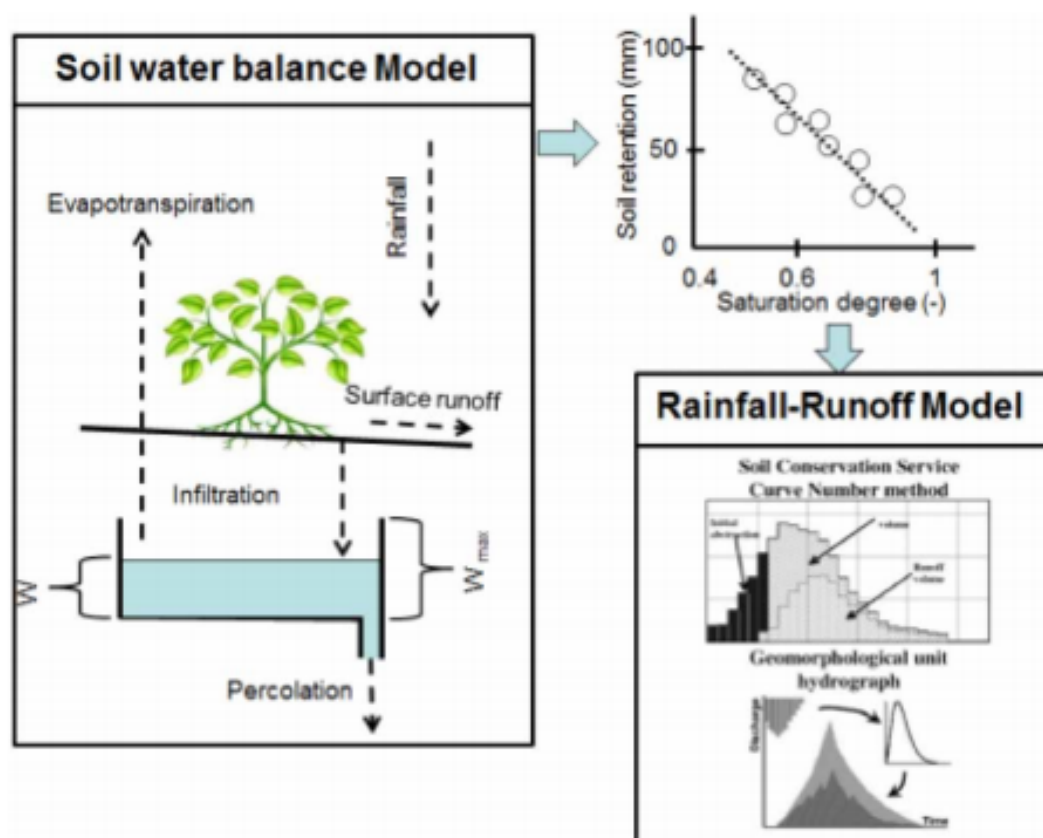
Figure 7: Structure of the MISDc model

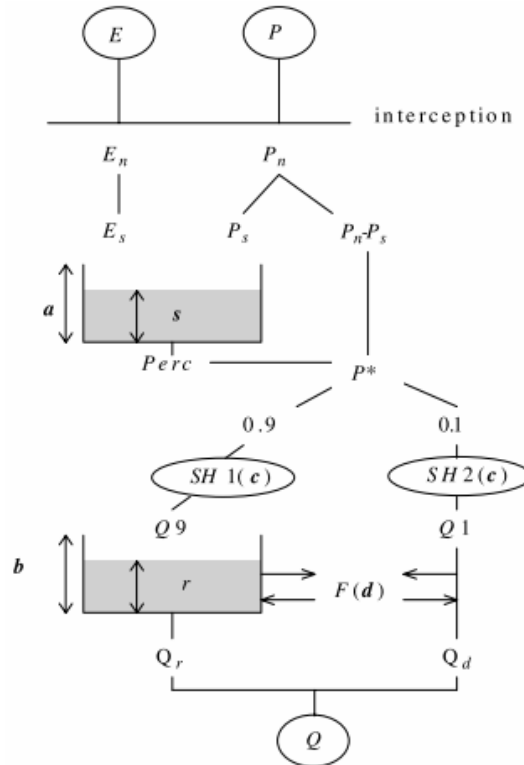*Table 3: Description of the parameters of the MISDc model parameters*

Parameters	Description	Unit	Range of values
Wp	Initial condition, fraction of Wmax	-	[0.1 0.9]
Wmax	Field capacity	Mm	[50 3000]
M2	Exponent of drainage		[1 20]
Ks	Ks parameter of infiltration and drainage	Mm	[0.01 40]
Nu	Fraction of drainage versus interflow	Days	[0 1]
Gamma1	Coefficient of the lag-time relationship		[0.5 7]
lambda	Initial abstraction coefficient		[0.0001 0.4]
Sr	Multiplicative coefficient for surface runoff		[0.5 20]

3.2.3 GR4J

Génie Rural à 4 Paramètres Journalier (GR4J) is a global conceptual model with 4 parameters (Table 4). The version used in this study is the standard one described in Perrin et al. (2003), applied in many basins across the world. The model combines two reservoirs for production and routing with a unit hydrograph. Figure 8 represents the diagram of the structure of the GR4J model. After a precipitation, the effective rain is expressed in two terms (Ps and Pn-Ps). The first fills the soil tank and the second is transferred to the outlet by the routing function. This transferred part is also divided in two; the first part (90%) is transferred by the unit hydrograph 1 (SH1) and is filling the routing tank and the second part (10%) contributes to

the direct runoff via the unit hydrograph 2 (SH2). The parameter X2 simulates the sub-surface exchanges. The simulated discharge is the sum of discharge generated by the two unit-hydrographs.


Figure 8: Description of the components of the GR4J model

Table 4: Description of the parameters of the GR4J model

Parameters	Description	Unit	Range of values
X1	Production reservoir capacity	Mm	[5 2000]
X2	Underground exchange coefficient	Mm	[-10 4]
X3	Daily capacity of the routing tank	Mm	[1 300]
X4	Base time of Unit Hydrograph	Days	[0 5]

3.2.4 CREST

The Coupled Routing and Excess Storage (CREST) model was first developed by Wang et al. (2011) and is a derivative of the Xinanjiang model which features a variable infiltration curve for partitioning rainfall into direct runoff and infiltration. CREST was designed as a distributed model developed by the University of Oklahoma (www.hydro.ou.edu) and the NASA SERVIR project (www.servir.net). The version used in this work is the lumped version (Figure 9) including two soil layers and 5 parameters (Table 5), and does not require distributed rainfall as input. The CREST model has been recently implemented in the Ensemble Framework For Flash Flood Forecasting (EF5) to issue flash flood warnings by the US National Weather Service (Flaming et al., 2020).
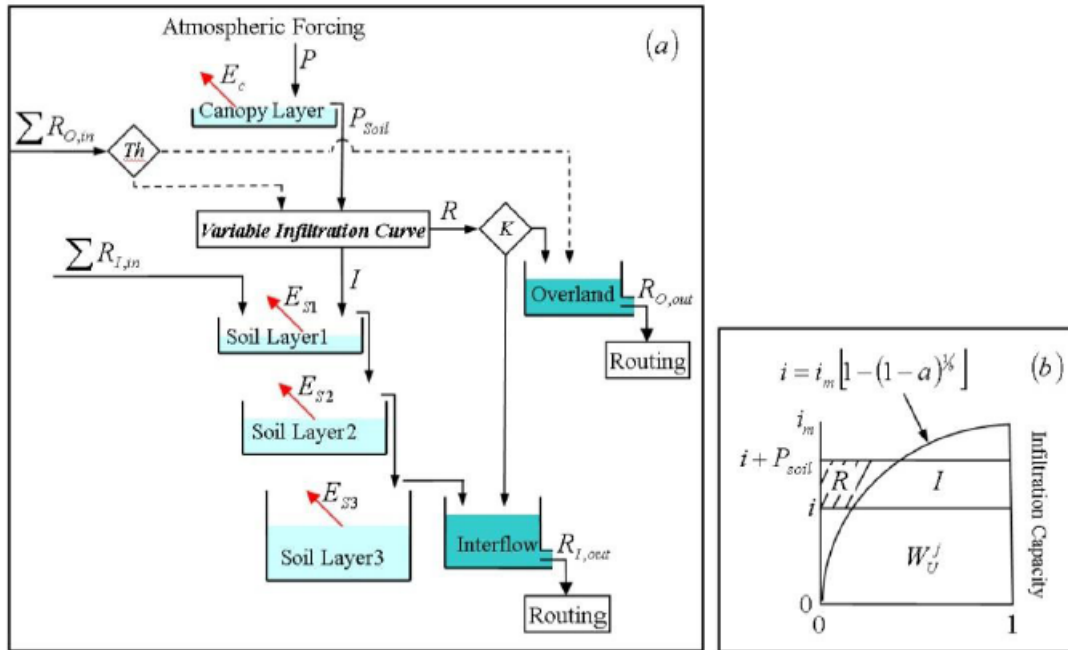
Figure 9: Diagram of the CREST model

Table 5: Description of the CREST parameters

| Parameters	Description	Unit	Range of values
P1	Maximum soil water storage capacity	mm	[0.1 1000]
P2	Hydraulic soil conductivity	Mm/h	[0.1 50]
P3	The overland reservoir discharge multiplier	-	[0 1]
P4	The interflow reservoir discharge multiplier	-	[0 1]
P5	The exponent of the variable infiltration curve	-	[0 100]

4. RESULTS

3.1 Ability of the different rainfall products to detect runoff events

The best correlations between runoff events and rainfall are obtained with the SM2RAIN and the H64 product (Figure 10), followed by GPM and H67. The largest number of significant correlations is obtained with the SM2RAIN (10 basins out of 12) and the H64 product (9 basins out of 12) as shown in Figure 11. Only the H64 product has positive correlations in all basins, followed by SM2RAIN for 11 out of 12 basins. For some basins, there are strong differences   in the correlations for events above the median and for more extreme runoff

events above the 95th percentile. These shows that the accuracy of the different product may differ from moderate to heavy rainfall events and any extrapolation should be evaluated carefully.
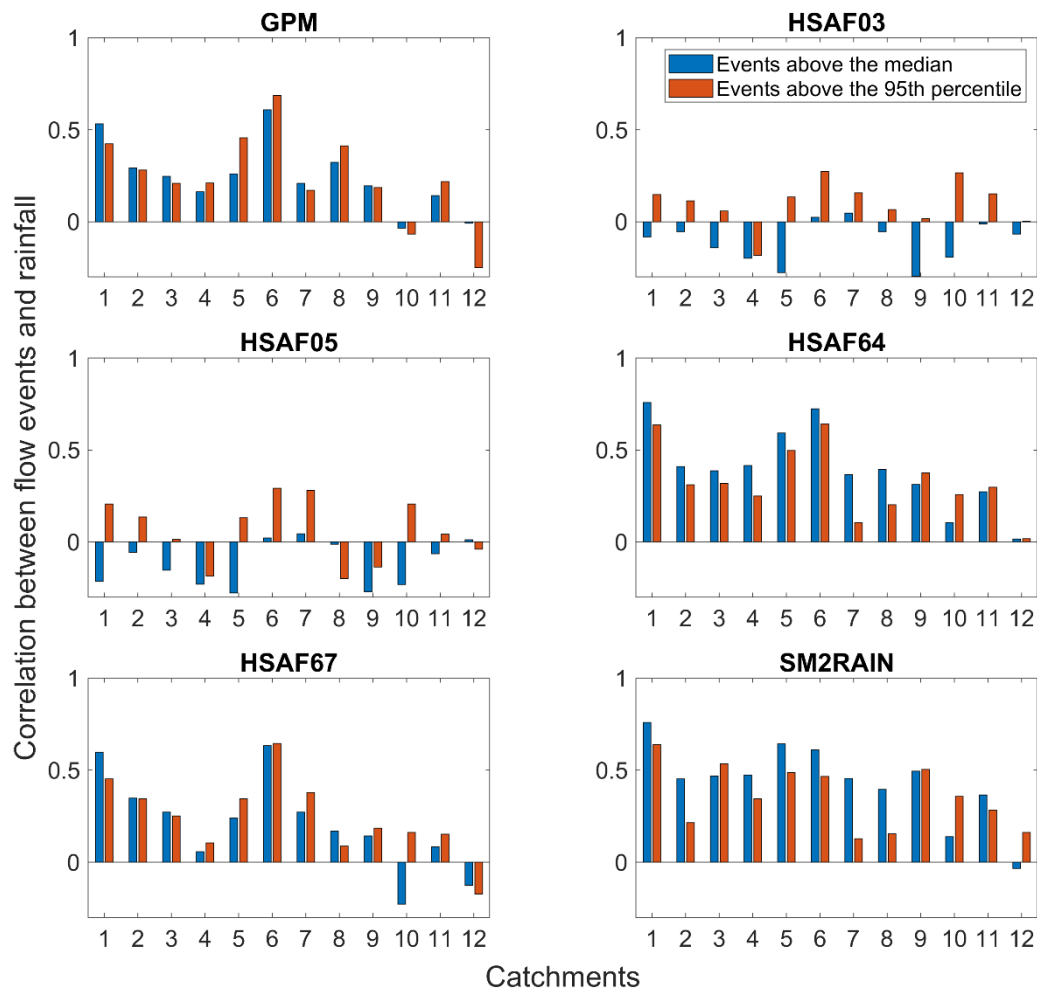
Figure 10: Correlation coefficient between flow events and corresponding event rainfall estimated from the different products
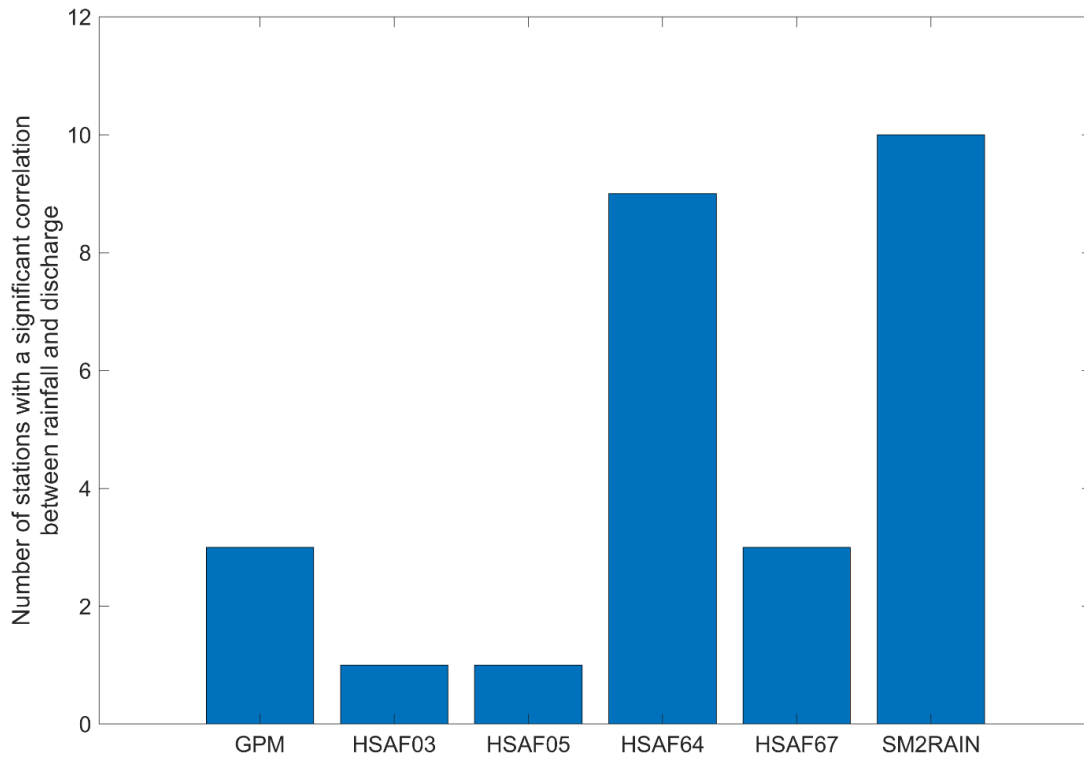
Figure 11: Number of stations with a significant correlation between flow event and rainfall from the different data products

## 3.2 Hydrological modelling with satellite rainfall products

On average, similar results to the event-based analysis are obtained with the hydrological model evaluation (Figure 12). The best results in terms of KGE values are obtained with SM2RAIN and H64, with KGE values consistently above 0. It should be noted that, on average, the KGE values remain small, with only for a few products a median value close to 0.5. Despite its increased use over different regions of the globe with satisfactory results, the GPM precipitation shows a rather strong variability in its efficiency to reproduce runoff depending on the basin and the hydrological model. The H03 and H05 precipitation products provide the least reliable simulations and notably in the case of the H03 product, a large variability of the results depending on the hydrological model.

The catchment-specific results shown in Figure 13 indicate that for some rainfall products, the most complex models, CREST and MISDc are able to compensate some of the bias of the rainfall data, as it is the case for H03. On the opposite, for the two most efficient products, SM2RAIN and H64, all the different models provide positive KGE criterions values. These

results highlight the importance of using different hydrological models when comparing different precipitation products and in particular hydrological models that are adapted to represent the local hydrological processes at play.
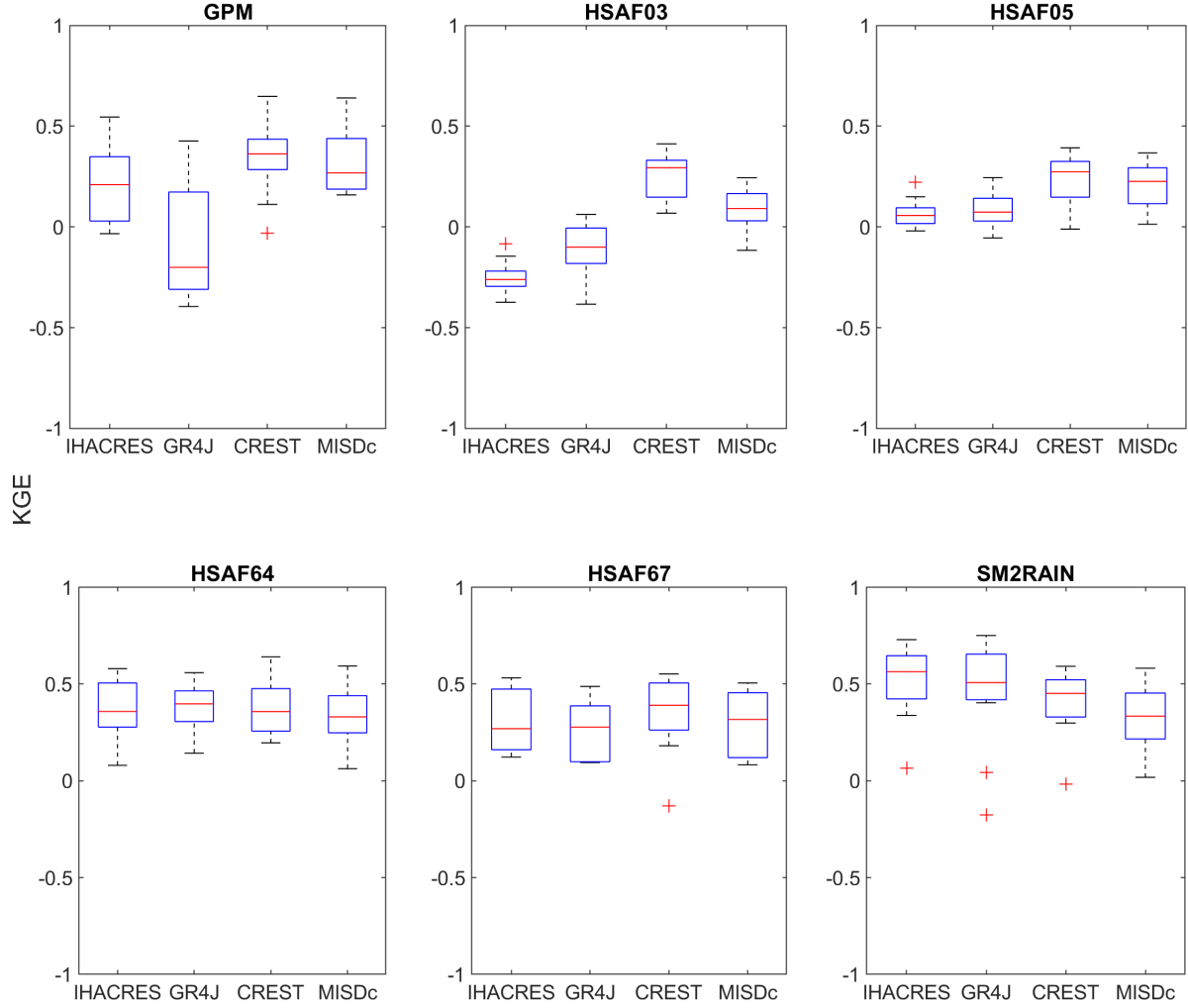

Figure 12: Calibration results of the different hydrological models (IHACRES, GR4J, CREST and MISDc) driven with the different precipitation products. The limits of the boxplots represent the 25th and 75th percentiles, with the line in the middle that refers to the median; the limits of the whiskers represent the 5th and 95th percentiles of KGE values.
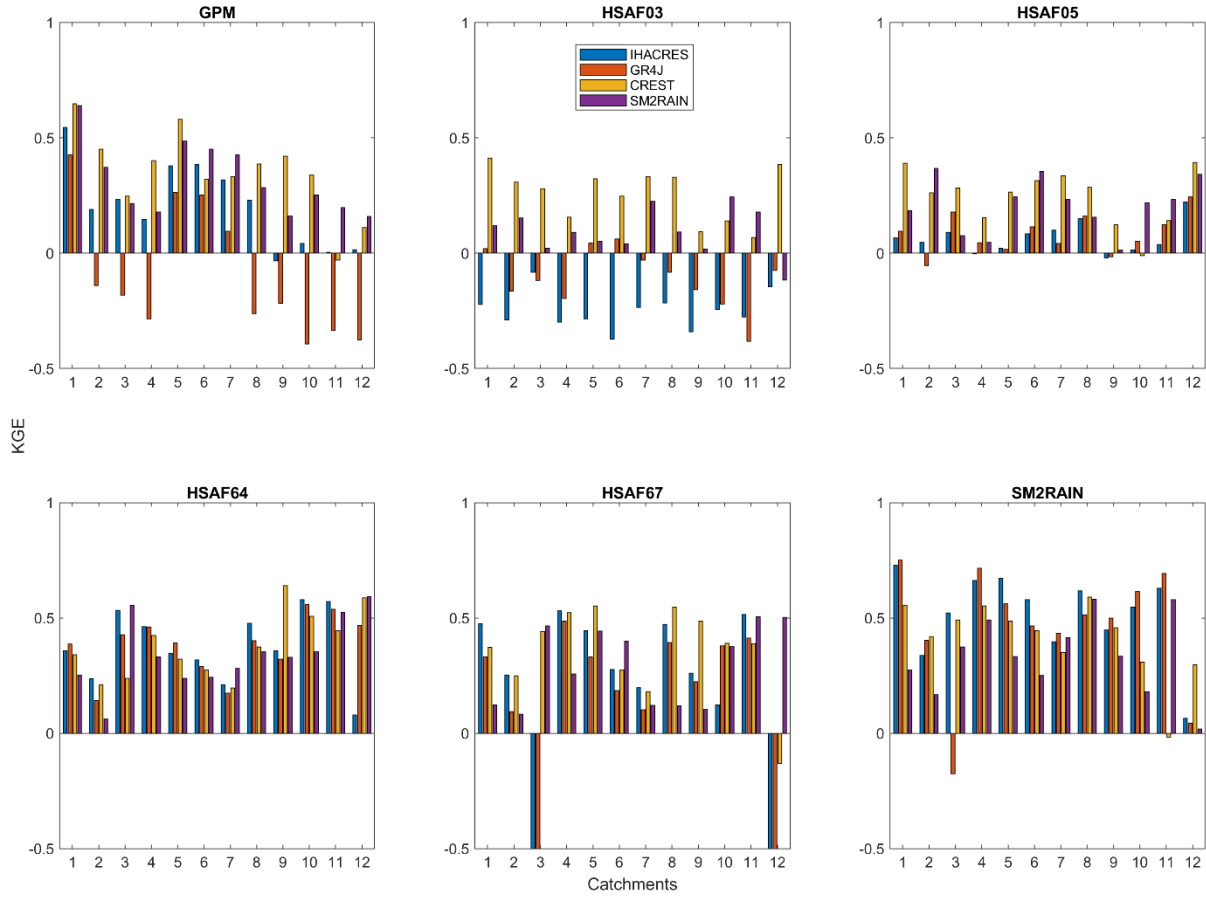
Figure 13: same as previous figure but with the KGE values for all catchments

In order to assess whether the results could be model-specific or depending on the catchments considered, the KGE values for each model have been averaged for each basin (Figure 14), and on the opposite, KGE values for each precipitation product obtained with different hydrological models have been also averaged (Figure 15). As shown on Figure 14, the results are consistent across the different catchments, with the SM2RAIN and H64 products outperforming the other ones with the highest averaged scores. The SM2RAIN product ranks the best in 8 catchments, H64 in 4 catchments. Similarly, it is interesting to investigate if the results could be model-specific, which would reduce the reliability of the assessment. As shown on Figure 15, in some cases some of the model structures considered may not be adapted to the catchment conditions. This is the case for the basins 3 and 12, located nearby in the middle Atlas Mountains. For these basins, the two most conceptual models, IHACRES and GR4J are not able to reproduce runoff when combined with some rainfall inputs, H03, H67 and to a lesser extent GPM and SM2RAIN. For these two basins, it is likely that the model structure of IHACRES and GR4J is less likely to adapt to the rainfall bias, maybe due to the mountainous nature of these basins. On average, the CREST model provides the best

stability in terms of performance across basins and rainfall products, with the best KGE values in 11 basins out of 12.
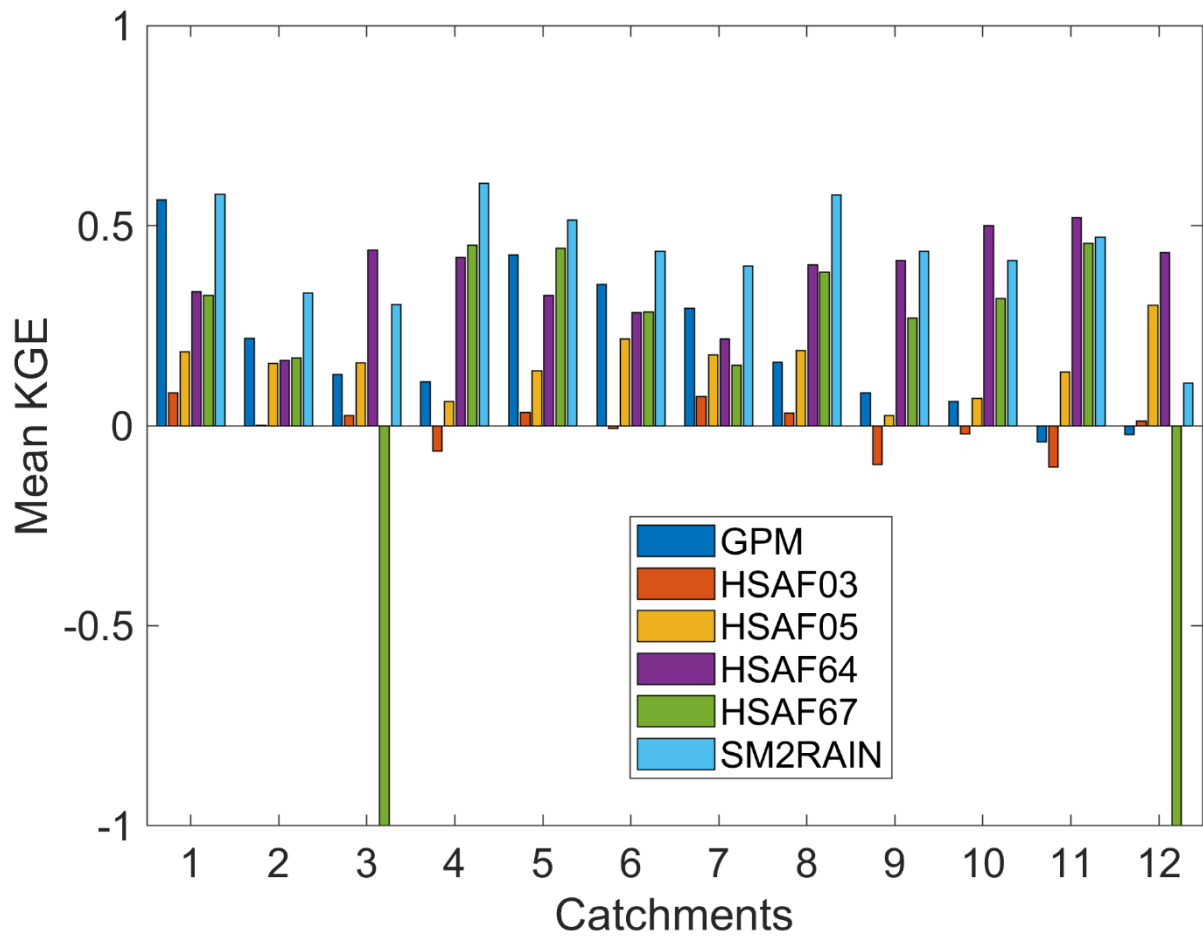

Figure 14: Calibration results aggregated by catchment for each precipitation product
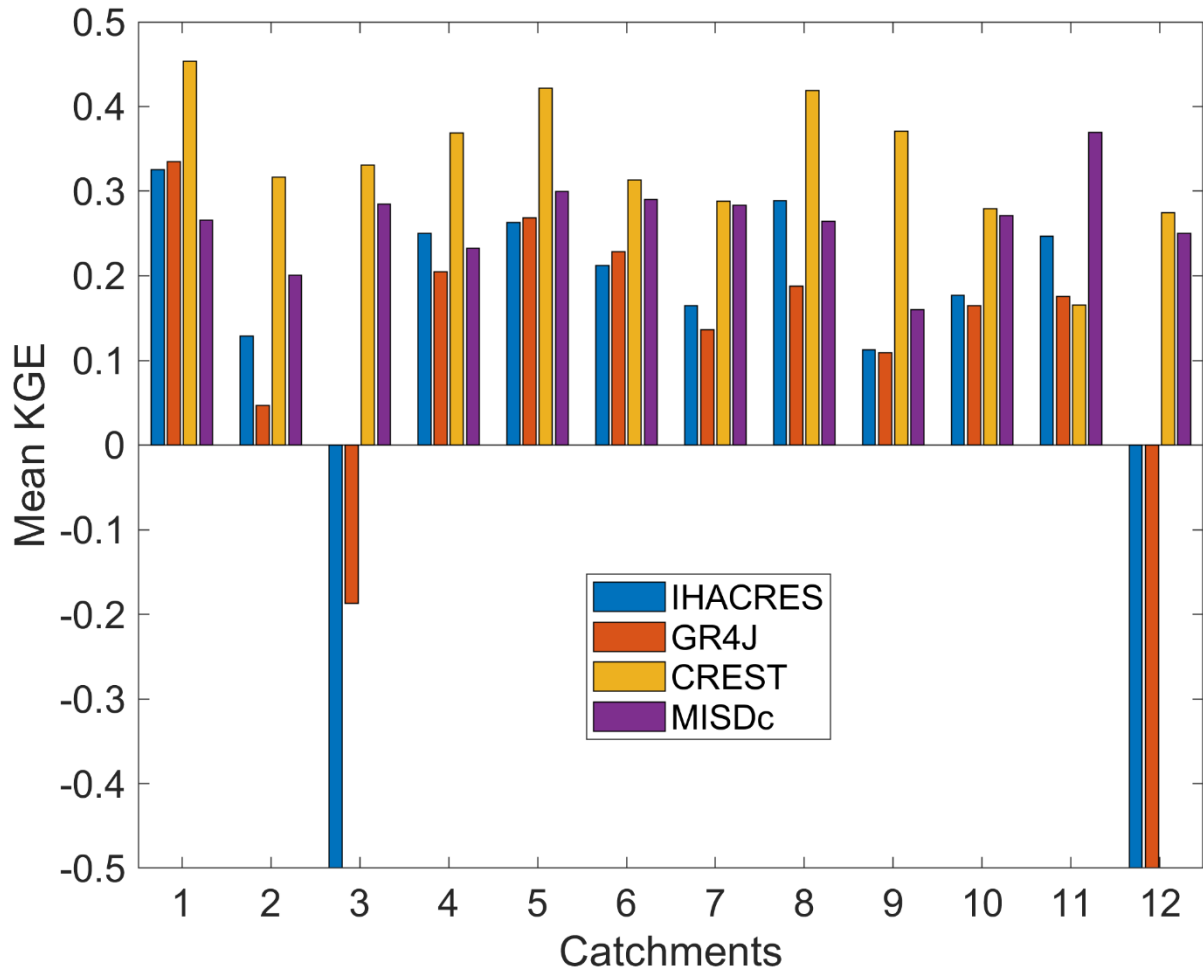
Figure 15: Calibration results aggregated by catchment for each hydrological model

Beside the analysis of model scores such as the KGE values, the analysis of simulated hydrographs could also provide interesting insights on the efficiency of the different rainfall products with the different hydrological models. For instance, as shown on Figure 16, both the peak runoff but also the recession parts following a high-flow event can be very different with different model structures. For instance, the CREST model seems to provide less steep recession curves in these basins when the GR4J model has difficulties to reproduce very low flows close to zero. Also, some spurious peaks could be simulated, as shown in the latter part of the hydrogram shown on Figure 16, due to the inherent bias of the different rainfall inputs. These results point out the need to evaluate carefully the choice of a particular hydrological model to perform simulations with satellite product, depending on the intended use (ie. reproduction of peak flows, low flows, or applications related to water resources management).
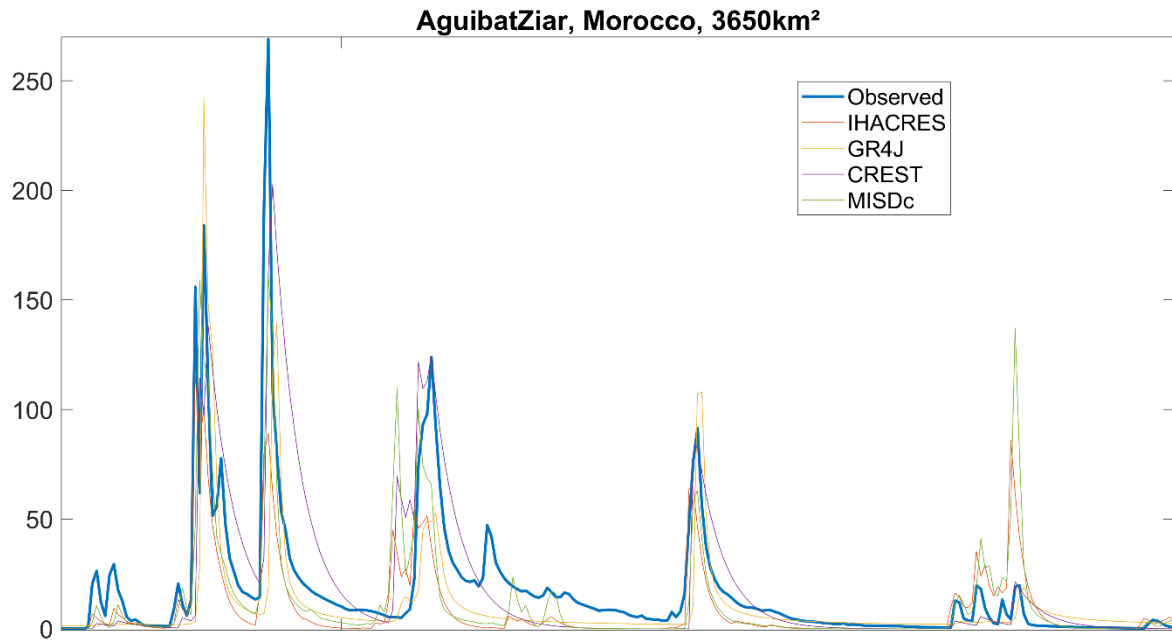
Figure 16: hydrographs for the AguibatZiar basin located in North Morocco, for the four hydrological models driven by GPM rainfall

3.3 Relationship with basins characteristics

In an attempt to link the rainfall products and model efficiency to reproduce runoff, the KGE values for the two best performing products, SM2RAIN and H64 have been related to the different catchment properties listed in Table 1. As shown in Figure 17, there is a different behavior for hydrological models driven by SM2RAIN or H64. The figure showing the mean KGE averaged over all models (IHACRES, GR4J, CREST, MISDc) indicates that for H64 there is a clear relationship with basins properties, with higher KGE in basins with a larger base flow contribution and lower flashiness. However, the relationship is inverse – or even non existing – with the SM2RAIN product. Similar results are obtained when looking at each hydrological model separately, showing that to a large extent the links with catchment properties are dependent on the precipitation product and the hydrological model. This analysis should be extended to a larger number of basins, with more contrasted properties in terms of catchment areas, range of elevation and climate characteristics, in order to derive more meaningful relationships.
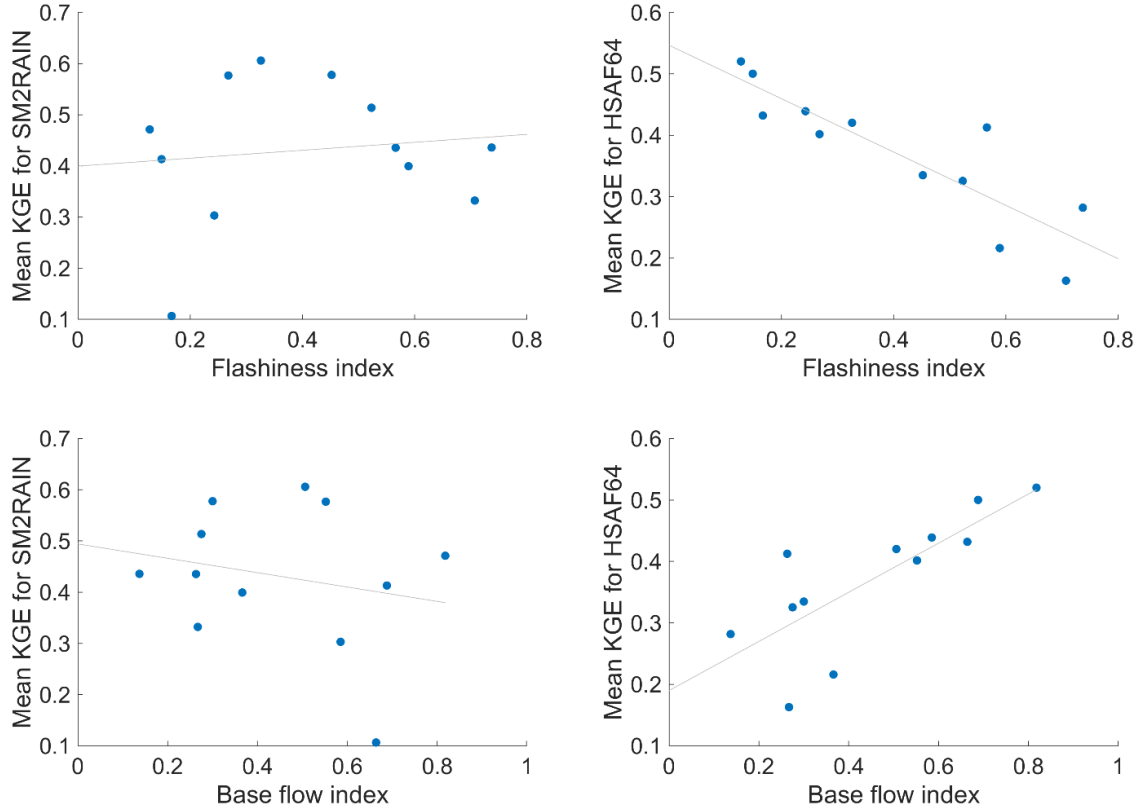
Figure 17: Relationships between mean KGE values obtained with the SM2RAIN (left) and H64 product (right) and catchment descriptors

3.4 Validation on independent data

With the perspective of using satellite precipitation data for operational applications, it would be necessary to validate the river discharge simulated with satellite rainfall on data that has not been used for calibrating the hydrological model, in order to estimate the extrapolation and prediction capabilities. A test was performed with the data available here for only 5 years, cutting the original data samples for each station into two calibration and validation samples of 2.5 years each. The results showed in the supplementary material (Figure S2) that such a short time period is not enough for a proper validation in such semi-arid environments characterized by a strong inter-annual variability of rainfall and runoff, with KGE values consistently below zero for the majority of cases. As shown on Figure 18, the hydrographs shapes are quite different from a year to another one, thus this division in two hydrological years only does not make it possible to have the calibrated model robust enough to adapt to the characteristics of the episodes in validation. Longer time series or event-based modelling

strategies (ie. modelling each sequence of runoff following a rainfall event separately) would be required to overcome this limitation.
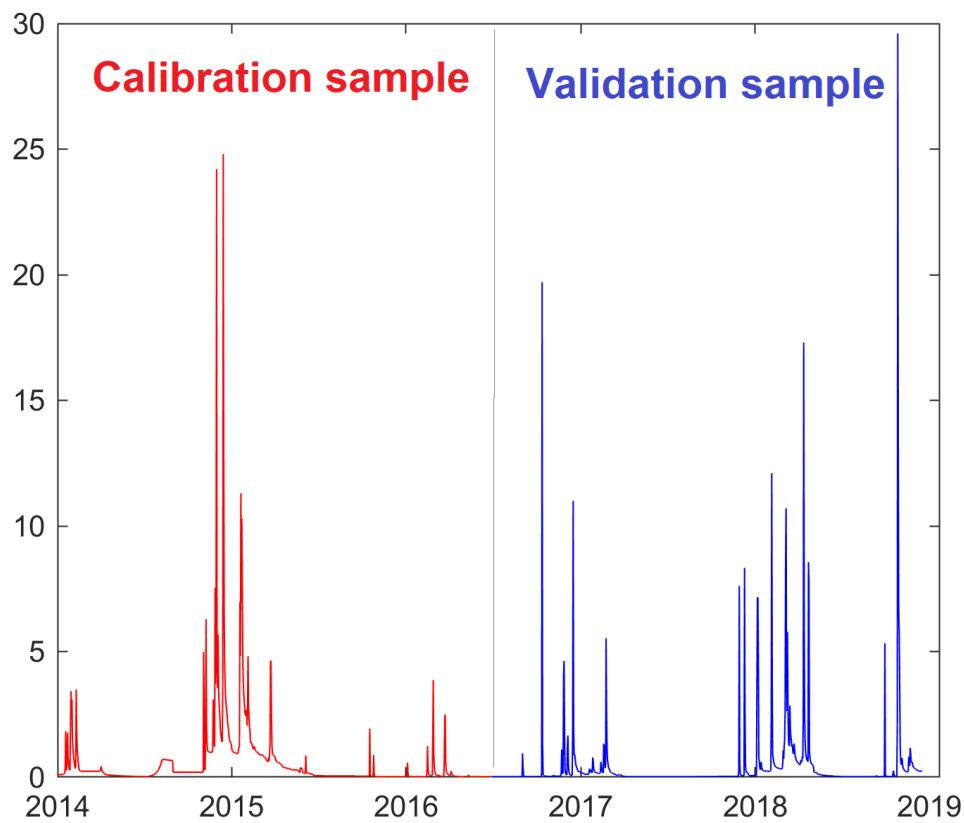
Figure 18: Example of the validation and calibration samples for AguibatZiar basin (January 2014 to June 2016 and July 2016 to December 2018)

4. CONCLUSIONS

This study relied on the collection of an unprecedented database over river basins located in Algeria, Morocco, Tunisia, when most previous satellite data assessments in this region were conducted only at the basin scale. Yet, data quality remains an issue, with uneven temporal coverage of the different records and spurious data detected in several cases. Consequently, after data quality screening, 12 basins were used in the analysis with sufficiently long time series to cover a recent period (2014-2018) when all precipitation products were available. However, since some rainfall products are covering different periods (example of SM2RAIN since 2007, GPM since 2000), it is possible to expand the analysis provided herein to longer time periods for the river basins having long discharge records.

The 6 different precipitation products tested in the present study are spanning the range of the "state-of-art" most recent remote sensing products for precipitation, obtained from different sensors. The best performances were observed with the two products assimilating soil moisture information, SM2RAIN and H64. The different precipitation product efficiency at reproducing river discharge was found quite homogeneous across the different catchments, beside the different accuracy of the hydrological models tested. Overall, due to the small number of basins it was difficult to derive any catchment specific recommendations. There is a global tendency towards a better efficiency of precipitation products in larger basins and with less arid conditions, but this would need to be further quantified using a larger set of basins with different characteristics.

The use of different hydrological models has shown that the assessment results are similar with the different models, indicating the performance of the different precipitation product is not dependent on the choice of the hydrological model. However, since different hydrological models may behave differently in basins with different characteristics, it is advised to properly select hydrological model(s) for a given application, for instance flood modelling or water resources assessment, since some model structure may be more adapted to reproduce runoff dynamics in a particular basin. Some model structures were found inadequate for a particular rainfall product and catchment.

Further work should aim at improving the representativeness of the results in a broader range of different catchments, according to the size, altitude range, land use and climatic conditions,

in order to provide guidelines towards the use of a particular rainfall product in a given hydro-climatic context. Furthermore, in an attempt to develop monitoring approaches tailored for operational application, there is a need to evaluate the rainfall products available at the hourly time steps to test threshold-based approaches for flood warning systems.

References

Baker, D.B., Richards, R.P., Loftus, T.T. and Kramer, J.W., 2004. A new flashiness index: Characteristics and applications to midwestern rivers and streams . JAWRA Journal of the American Water Resources Association, 40(2), pp.503-522.

Beria, H., Nanda, T., Bisht D.S., Chatterjee, C., 2017. Does the GPM mission improve the systematic error component in satellite rainfall estimates over TRMM? An evaluation at a pan-India scale. Hydrol Earth Syst Sci 21:6117–6134.

Brocca, L., Melone, F. and Moramarco, T., 2008. On the estimation of antecedent wetness conditions in rainfall–runoff modelling. Hydrological Processes, 22(5), pp.629-642.

Brocca, L., Liersch, S., Melone, F., Moramarco, T., and Volk, M., 2013. Application of a model-based rainfall-runoff database as efficient tool for flood risk management, Hydrol. Earth Syst. Sci., 17, 3159–3169, https://doi.org/10.5194/hess-17-3159-2013.

Brocca, L., Ciabatta, L., Massari, C., Moramarco, T., Hahn, S., Hasenauer, S., Kidd, R., Dorigo, W., Wagner, W., and Levizzani, V., 2014. Soil as a natural rain gauge: estimating global rainfall from satellite soil moisture data, J. Geophys. Res., 119, 9, 5128–5141, https://doi.org/10.1002/2014JD021489.

Croke, B.F.W., Jakeman, A.J., 2004. A catchment moisture deficit module for the IHACRES rainfall-runoff model. Environ. Model. Softw. 19, 1–5.

El Khalki M., Tramblay Y., Massari C., Brocca L., Simmoneaux V., Gascoin S., Saidi E.M., 2020. Challenges in flood modelling over data scarce regions: how to exploit globally available soil moisture products to estimate antecedent soil wetness conditions in Morocco. Natural Hazards and Earth System Sciences, 20, 2591–2607, https://doi.org/10.5194/nhess-20-2591-2020.

El Khalki E.M., Tramblay Y., Saidi E.M., Bouvier C., Hanich L., Benrhanem M., Alaouri M., 2018. Comparison of modelling approaches for flood forecasting in the High-Atlas Mountains of Morocco. Arabian Journal of Geosciences 11, 410. https://doi.org/10.1007/s12517-018-3752-7

Er-Raki, S., et al., 2010. Assessment of reference evapotranspiration methods in semi-arid regions: can weather forecast data be used as alternate of ground meteorological parameters? Journal of Arid Environments, 74, 1587–1596. doi:10.1016/j.jaridenv.2010.07.002

Flamig, Z. L., Vergara, H., and Gourley, J. J.: The Ensemble Framework For Flash Flood Forecasting (EF5) v1.2: description and case study, Geosci. Model Dev., 13, 4943–4958, https://doi.org/10.5194/gmd-13-4943-2020, 2020.

Hou, A. Y., Kakar, R. K., Neeck, S., Azarbarzin, A. A., Kummerow, C. D., Kojima, M., … Iguchi, T., 2014. The global precipitation measurement mission. Bulletin of the American Meteorological Society, 95(5), 701–722.

Kling, H., Fuchs, M., and Paulin, M., 2012. Runoff conditions in the upper Danube basin under an ensemble of climate change scenarios, J. Hydrol., 424, 264–277, https://doi.org/10.1016/j.jhydrol.2012.01.011

Nguyen, T.H., Masih, I., Mohamed, Y.A., Van Der Zaag, P., 2018. Validating rainfall-runoff modelling using satellite-based and reanalysis precipitation products in the Sre Pok catchment, the Mekong River basin. Geosciences 8(5):164–184. https://doi.org/10.3390/geosciences8050164.

Perrin, C., Michel, C., Andréassian, V., 2003. Improvement of a parsimonious model for streamflow simulation. J. Hydrol. 279, 275–289.https://doi.org/10.1016/S0022-1694(03)00225-7.

Saouabe, T., El Khalki, E. M., Saidi, M. E. M., Najmi, A., Hadri, A., Rachidi, S., … Tramblay, Y. 2020 Evaluation of the GPM-IMERG Precipitation Product for Flood Modeling in a Semi-Arid Mountainous Basin in Morocco. Water, 12(9), 2516. doi:10.3390/w12092516

Tarasova, L., Basso, S., Wendi, D., Viglione, A., Kumar, R., & Merz, R. (2020). A process-based framework to characterize and classify runoff events: The event typology of Germany. Water Resources Research, 56, e2019WR026951. https://doi.org/10.1029/2019WR026951

Thiemig, V., Rojas, R., Zambrano-Bigiarini, M., & De Roo, A. (2013). Hydrological evaluation of satellite-based rainfall estimates over the Volta and Baro-Akobo Basin. Journal of Hydrology, 499, 324-338.

Tramblay, Y., R. Bouaicha, L. Brocca, W. Dorigo, C. Bouvier, S. Camici, and E. Servat. 2012. Estimation of Antecedent Wetness Conditions for Flood Modelling in Northern Morocco. Hydrology and Earth System Sciences 16 (11): 4375–86. https://doi.org/10.5194/hess-16-4375-2012 .

Tramblay Y., Thiemig V., Dezetter A., Hanich L., 2016. Evaluation of satellite-based rainfall products for hydrological modelling in Morocco, Hydrological Sciences Journal 61(14), 2509-2519. http://dx.doi.org/10.1080/02626667.2016.1154149

UK Institute of Hydrology, 1980. Low Flow Studies. Reports. Institute of Hydrology.

Van der Knijff, J. M., Younis, J. and de Roo, A. P. J., 2010. LISFLOOD: A GIS-based distributed model for river basin scale water balance and flood simulation, Int. J. Geogr. Inf. Sci., 24(2), 189–212.

Wang, Jiahu; Hong, Yang; Li, Li; Gourley, Jonathan J.; Khan, Sadiq I.; Yilmaz, Koray K.; Adler, Robert F., Policelli, Frederick S.; Habib, Shahid; Irwn, Daniel; Limaye, Ashutosh S.; Korme, Tesfaye; Okello, Lawrence; 2011. The coupled routing and excess storage (CREST) distributed hydrological model. Hydrological Sciences Journal, 56, 84–98. 10.1080/02626667.2010.543087

ANNEXES

Annex 1: List of the 41 basins with daily discharge data

Basin	Country	Centroid Longitude	Centroid Latitude	Area [km²]
Aguibate Ezziar	Morocco	-6,45	33,75	3655
Ain Loudah	Morocco	-6,35	33,55	698
Aissi	Algeria	4,05	36,55	431
Ait Ouchène	Morocco	-6,05	32,25	2400
Azib Sultane	Morocco	-5,45	34,15	16051
Basin10	Tunisia	9,25	37,05	453
Basin1	Tunisia	9,65	37,15	76
Basin2	Tunisia	9,25	36,85	159
Basin3	Tunisia	9,55	36,15	1180
Basin4	Tunisia	8,25	36,45	361
Basin5	Tunisia	8,35	35,75	2655
Basin6	Tunisia	8,15	36,25	825
Basin7	Tunisia	9,15	35,85	2168
Basin8	Tunisia	9,25	35,75	675
Basin9	Tunisia	8,85	35,75	795
Belksiri	Morocco	-6,05	34,55	0,78
Boukdir	Algeria	2,25	36,45	76
Chachanmellah	Morocco	-5,65	32,65	1422
Had Kourt	Morocco	-5,75	34,55	8
Idriss1er	Morocco	-4,75	34,05	3600
Isser	Algeria	2,95	36,15	3615
Lalla Chafia	Morocco	-6,35	33,35	2232
Malah Est	Algeria	3,25	36,15	274
Ras ElFathia	Morocco	-6,55	33,05	3504
Ratba	Morocco	-4,95	34,85	467
Sidi Jabeur	Morocco	-6,85	33,55	11
Sidi Mly Cherif	Morocco	-6,65	33,25	646

Taghzout	Morocco	-5,85	32,55	171
Tagzirt	Morocco	-6,35	32,45	431
Tamchachat	Morocco	-5,15	33,05	133
Tarhat	Morocco	-5,55	33,05	1012
Nfis	Morocco	-8,75	30,95	1290
Sidi Bouathman	Morocco	-8,25	31,15	519
Illoudjane	Morocco	-7,45	31,45	571
Rheraya	Morocco	-7,75	31,15	225
Ourika	Morocco	-8,85	31,05	503
Ghdat	Morocco	-7,55	31,25	551
Zat	Morocco	-8,55	30,95	521
Sidi Hsain	Morocco	-7,95	31,05	109
Tillouguite	Morocco	-6,25	32,05	2500
Zddine	Algeria	1,85	35,95	418
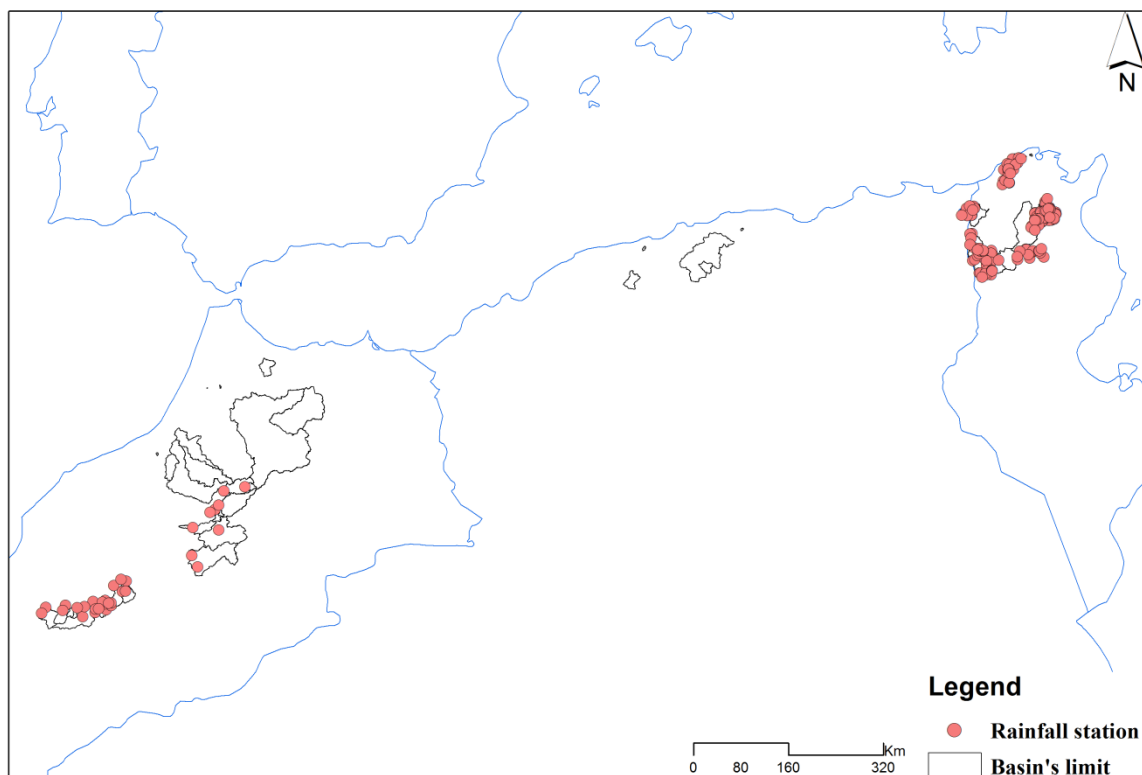
Figure S1: Location of the available rainfall stations
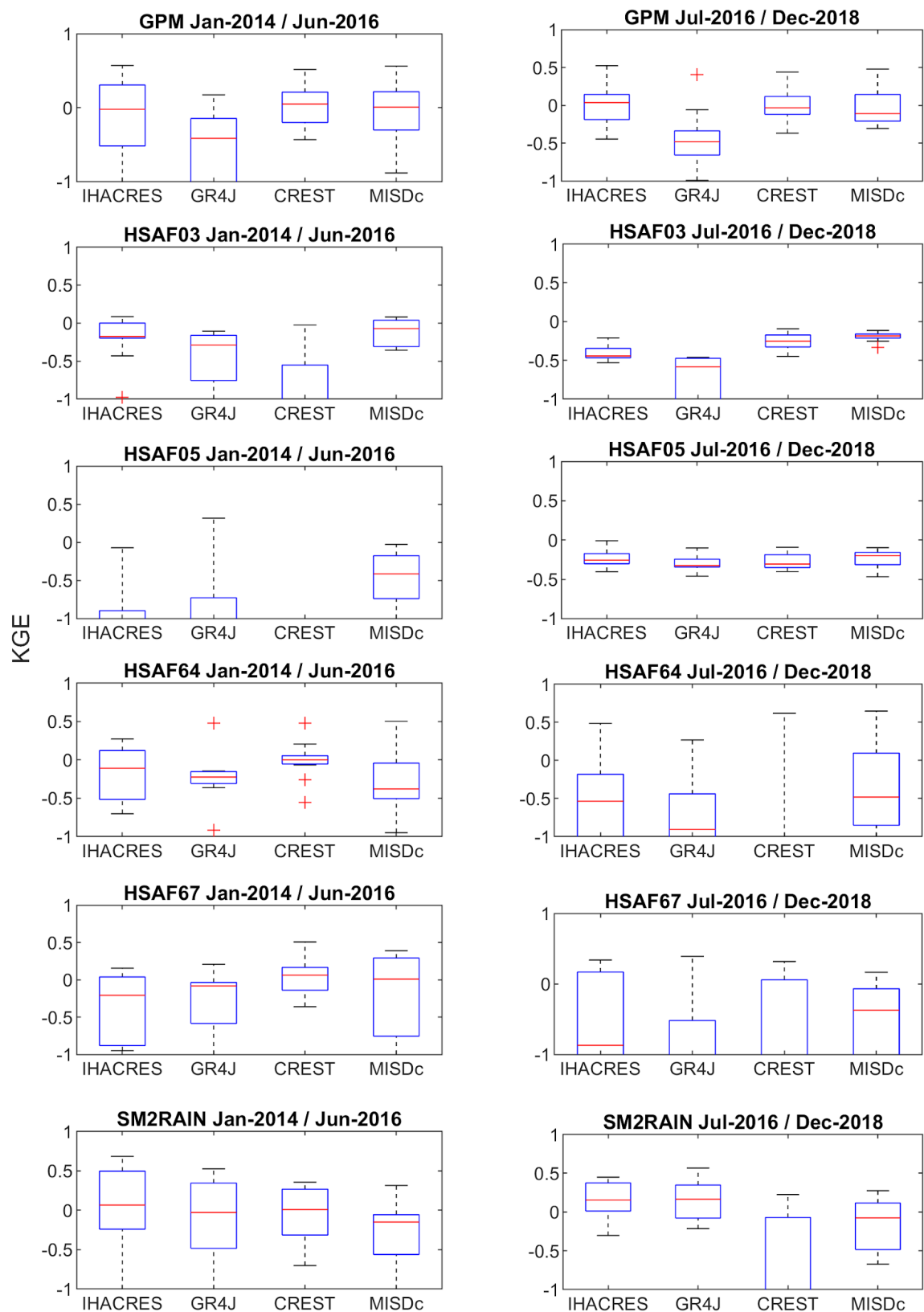
Figure S2   : validation results on two sub-periods, January 2014 to June 2016 and July 2016 to December 2018.